END
DATE
FILMED
8
DTIC

| 1.0 | | 2.8 | 2.5 |
|---|---|---|---|
| | | 3.2 | 2.2 |
| | | 36 | |
| | | 40 | 2.0 |
| 1.1 | | | |
| | | | 1.8 |
| 1.25 | 1.4 | | 1.6 |

MICROCOPY RESOLUTION TEST CHART

NATIONAL BUREAU OF STANDARDS 1963 A

AD A092961

| REPORT DOCUMENTATION PAGE | | READ INSTRUCTIONS BEFORE COMPLETING FORM |
|---|---|---|
| 1. REPORT NUMBER<br><br>NRL Memorandum Report 4389 | 2. GOVT ACCESSION NO.<br><br>AD-A092 961 | 3. RECIPIENT'S CATALOG NUMBER<br><br>AD- |
| 4. TITLE (and Subtitle)<br>NUMERICAL SIMULATIONS OF EQUATORIAL SPREAD F USING ALTAIR INCOHERENT BACKSCATTER MEASURED ELECTRON DENSITY PROFILES FROM THE 17 JULY 1979 DNA KWAJALEIN CAMPAIGN | | 5. TYPE OF REPORT & PERIOD COVERED<br>Interim report on a continuing NRL problem. |
| | | 6. PERFORMING ORG. REPORT NUMBER |
| 7. AUTHOR(s)<br><br>S. T. Zalesak and S. L. Ossakow | | 8. CONTRACT OR GRANT NUMBER(s) |
| 9. PERFORMING ORGANIZATION NAME AND ADDRESS<br>Naval Research Laboratory<br>Washington, DC 20375 | | 10. PROGRAM ELEMENT, PROJECT, TASK AREA & WORK UNIT NUMBERS<br><br>67-0889-0-0 |
| 11. CONTROLLING OFFICE NAME AND ADDRESS<br>Defense Nuclear Agency<br>Washington, DC 20305 | | 12. REPORT DATE<br>December 3, 1980 |
| | | 13. NUMBER OF PAGES<br>28 |
| 14. MONITORING AGENCY NAME & ADDRESS(if different from Controlling Office) | | 15. SECURITY CLASS. (of this report)<br><br>UNCLASSIFIED |
| | | 15a. DECLASSIFICATION/DOWNGRADING SCHEDULE |

16. DISTRIBUTION STATEMENT (of this Report)

Approved for public release; distribution unlimited.

17. DISTRIBUTION STATEMENT (of the abstract entered in Block 20, if different from Report)

19. KEY WORDS (Continue on reverse side if necessary and identify by block number)
Equatorial Spread F
Numerical simulations
Collisional Rayleigh-Taylor mechanism
ALTAIR electron density profiles
Spread F bubbles

20. ABSTRACT (Continue on reverse side if necessary and identify by block number)
Using electron density profiles measured by the ALTAIR radar on 17 July 1979, we have performed global large scale size numerical simulations of the nonlinear evolution of the collisional Rayleigh-Taylor instability in the equatorial ionosphere. The ALTAIR profiles were taken approximately four and one-half hours prior to the launch of a rocket equipped with plasma diagnostics instrumentation, and on the order of one hour prior to the onset of equatorial spread F. Using 5% amplitude sinusoidal initial perturbations in our numerical simulations, we find fully developed spread F bubbles (plumes) on time scales of approximately one-half hour for both small (8 km) and large (200 km) horizontal scale lengths.

DD FORM 1473 EDITION OF 1 NOV 65 IS OBSOLETE
1 JAN 73
S/N 0102-LF-014-6601

i

# CONTENTS

| Accession For | | |
|---|---|---|
| NTIS GRA&I | ☒ | |
| DDC TAB | ☐ | |
| Unannounced | | |
| Justification_____ | | |
| By_____ | | |
| Distribution/ | | |
| Availability Codes | | |
| Dist. | Avail and/or special | |
| A | | |

# NUMERICAL SIMULATIONS OF EQUATORIAL SPREAD F USING ALTAIR INCOHERENT BACKSCATTER MEASURED ELECTRON DENSITY PROFILES FROM THE 17 JULY 1979 DNA KWAJALEIN CAMPAIGN

## I.    INTRODUCTION

During the 17 July 1979 DNA PLUMEX I experiment, coordinated measurements of equatorial spread F (ESF) by radar backscatter using the ALTAIR radar, by plasma diagnostics using in situ rocket probes, and by scintillation measurements using the DNA Wideband satellite, were carried out.  Prior to the rocket launches, however, ALTAIR was used to monitor the equatorial environment into which the rockets would be launched.  In particular, off-perpendicular "incoherent" scans were made, giving direct profiles of electron density versus altitude, as well as coherent backscatter measurements.  Using a background laminar electron density profile of this type, taken before the onset of spread F, as the ambient laminar ionospheric profile, we have performed numerical simulations of the nonlinear evolution of the collisonal Rayleigh-Taylor instability.  This phenomenon is believed to be the cause[1-5] on the large scale irregularities during ESF.

Our results indicate fully developed spread F plumes (bubbles) on time scales of approximately half an hour, using initial sinusoidal perturbations of 5% amplitude and two different horizontal wavelengths (8 km and 200 km). ALTAIR radar and ionosonde data indicate  fully developed spread F approximately one hour after the aforementioned profile was taken[6].  The difference in times could easily be accounted for simply by assuming a smaller initial perturbation, i.e., the present measurements do not provide us with all the pertinent initial conditions prior to ESF onset.  Other factors, such as significant differences between local and magnetic field line integrated Pedersen conductivities, the shorting effects of background E region conductivities, and the effect of inertial terms in the ion momentum equation (ignored in our simulations) could also delay the progress of the instability.

1

Notwithstanding these effects, our aim was to show that these types of global large scale numerical simulations of the collisional Rayleigh-Taylor mechanism are consistent with the onset time and morphology of ESF during the 17 July 1979 campaign. Also, we find that the larger horizontal scale length bubbles consist of plasma which originated at much lower altitudes than that of their smaller horizontal scale length counterparts, resulting in much more depleted bubbles in the larger horizontal scale length case. This last effect is explained using scaling arguments similar to those which apply to the fringe field at the edge of a parallel plate capacitor.[5]

In Section II we briefly review the relevant theory and equations used in the numerical simulations; in Section III we present and analyze the numerical results; and in Section IV a summary is presented.

## II. THEORY

For a complete description of our theoretical and numerical model of the equatorial spread F phenomenon see reference 4. Briefly, we assume that the magnetic field line integrated Pedersen conductivity in the equatorial ionosphere is dominated by, and is therefore proportional to, the local (equatorial) Pedersen conductivity, which in turn is proportional to the product of the local ion-neutral collision frequency and the local electron density. This enables us to carry out our simulations in a two dimensional $(x,y)$ coordinate system. The constant magnetic field $\underline{B}$ is aligned along the $\hat{z}$ axis (pointing north). Gravity is directed along the negative $\hat{y}$ axis. $n(y)$, $\nu_R(y)$, and $\nu_{in}(y)$ are the ambient electron density, recombination coefficient, and ion-neutral collision frequency respectively. Magnetic field lines are assumed to terminate at both ends in an electrically

insulated medium (currents must close in the two dimensional plane, not in some distant E region).

Following reference 4, we describe the system with the two-fluid plasma continuity and momentum equations:

$$\frac{\partial n_\alpha}{\partial t} + \nabla \cdot (n_\alpha \underline{v}_\alpha) = - \nu_R n_\alpha \qquad (1)$$

$$\left(\frac{\partial}{\partial t} + \underline{v}_\alpha \cdot \nabla\right) \underline{v}_\alpha = \frac{q_\alpha}{m_\alpha} \left(\underline{E} + \frac{\underline{v}_\alpha \times \underline{B}}{c}\right) + \underline{g} - \nu_{\alpha n}(\underline{v}_\alpha - \underline{U}_n) \qquad (2)$$

where the subscript $\alpha$ denotes the species (i for ions, e for electrons), n is the species number density, $\underline{v}$ is velocity, $\nu_R$ is the recombination coefficient, $\underline{E}$ is the electric field, $\underline{g}$ is the gravitational acceleration, q is the species charge, $\nu_{\alpha n}$ is the species collision frequency with the neutral atmosphere, $\underline{U}_n$ is the neutral wind velocity, c is the speed of light, and m is the species mass.

Note that, in contrast to reference 4, we have dropped the term $+ \nu_R n_{\alpha o}$ from (1). This is the equivalent of dropping the assumption of the existence of an ionization source given by that term. This ionization source was such that the ambient ionization profiles $n_{\alpha o}(y)$ was an equilibrium profile ($\partial n_{\alpha o}/\partial t = 0$). Our present model therefore has instead

$$\frac{\partial n_{\alpha o}}{\partial t} = - \nu_R n_{\alpha o} \qquad (3)$$

3

Hence, when normalized results $n_\alpha(x,y)/n_{\alpha o}(y)$ are later presented, it should be understood that both the numerator and denominator are time dependent.

Figure 1 shows the recombination rate $\nu_R$ and ion-neutral collision frequency $\nu_{in}$ used in our simulations. It shall be seen presently that $\nu_{en}$ need not be specified as long as it is much smaller than the electron gyro-frequency $\Omega_e$. For details on the form of $\nu_{in}$ and $\nu_R$ as depicted in Figure 1, see reference 4. If we neglect the inertial terms (the left-hand side) of (2) by assuming the inertial time scales are much larger than either the gyro-periods or the mean time between collisions, then the equation can be inverted to give an algebraic expressions for $\underline{v}_\alpha$. In two-dimensional (x,y) geometry with $\underline{B}$ along the $\hat{z}$ axis, the solution is for our problem, with $m_e \ll m_i$, $\nu_{in}/\Omega_i \ll 1$, $\nu_{en}/\Omega_e = 0$ (where $\Omega_\alpha = eB/m_\alpha c$), and $\underline{U}_n = 0$,

$$\underline{v}_e = \frac{c}{B} \underline{E} \times \hat{z}, \quad \hat{z} = \frac{\underline{B}}{|\underline{B}|} \tag{4}$$

$$\underline{v}_i = \left( \frac{\underline{g}}{\Omega_i} + \frac{c}{B} \underline{E} \right) \times \hat{z} + \frac{\nu_{in}}{\Omega_i} \left( \frac{\underline{g}}{\Omega_i} + \frac{c}{B} \underline{E} \right) \tag{5}$$

We now make the electrostatic approximate,

$$\underline{E} = \nabla_\perp \phi \tag{6}$$

where $\nabla_\perp \equiv \hat{x}(\partial/\partial x) + \hat{y}(\partial/\partial y)$, and the quasi-neutrality approximation $n_e \approx n_i \equiv n$. We then have

$$\nabla_\perp \cdot \underline{j} = 0 \tag{7}$$

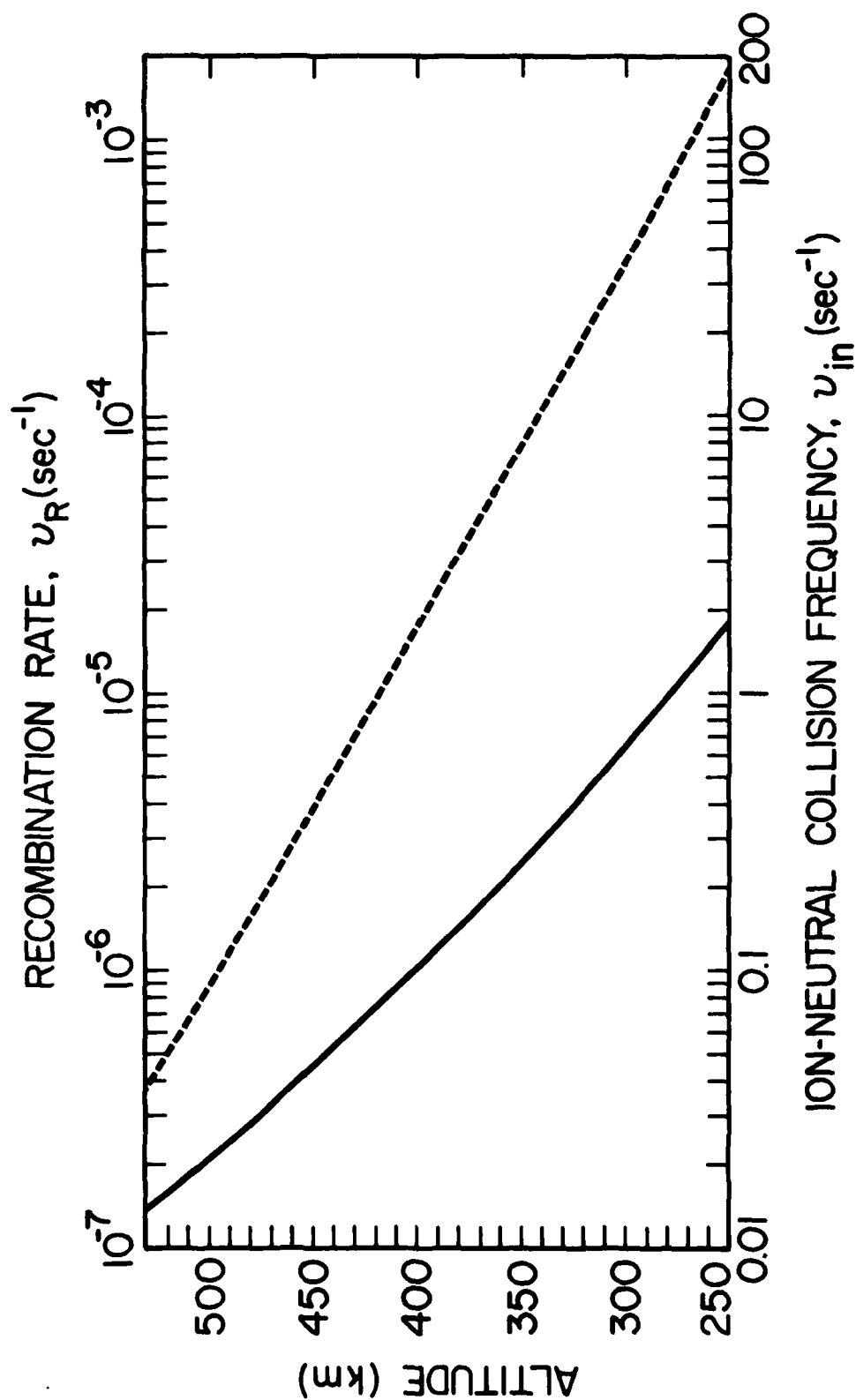$$\underline{j} \equiv en \, (\underline{v}_i - \underline{v}_e) \tag{8}$$

4

Fig. 1 — Ion-neutral collision frequency (solid line) $\nu_{in}$ and recombination coefficient (rate) $\nu_R$ as a function of altitude

Substituting (4) and (5) into (8) and evaluating (7), we have for the electrostatic potential:

$$\nabla_{\perp} \cdot (\nu_{in} n \, \nabla_{\perp} \phi) = - \frac{m_i}{e} g \frac{\partial}{\partial y} (\nu_{in} n) - \frac{B}{c} g \frac{\partial n}{\partial x} \qquad (9)$$

As in reference 4 we set $\phi = \phi_0 + \phi_1$ where $\nabla_{\perp} \phi_0 = - (m_i g/e) \, \hat{y}$. Since $\nabla_{\perp}^2 \phi_0 = 0$, our final potential equation becomes

$$\nabla_{\perp} \cdot (\nu_{in} n \, \nabla_{\perp} \phi_1) = - \frac{Bg}{c} \frac{\partial n}{\partial x} \qquad (10)$$

The effect of $\phi_0$ is merely to superimpose a bulk westward plasma velocity $g/\Omega_i$ on the electron velocity field determined from $\phi_1$, without affecting the morphology of the developing structures. Hence, we ignore this motion. In addition, we have ignored any upward or downward bulk motion of the ionospheric plasma, i.e., any ambient eastward or westward electric field. This is done because we have chosen a starting time for our simulation, which while prior to ESF onset, which coincides[6] with essentially no upward or downward bulk motion of the ionospheric plasma.

Our assumption of quasi-neutrality has made one of our two continuity equations (1) redundant. We therefore choose the electron equation for its simplicity:

$$\frac{\partial n}{\partial t} - \frac{\partial}{\partial x} \left( \frac{nc}{B} \frac{\partial \phi_1}{\partial y} \right) + \frac{\partial}{\partial y} \left( \frac{nc}{B} \frac{\partial \phi_1}{\partial x} \right) = - \nu_R n \qquad (11)$$

## III. NUMERICAL SIMULATION RESULTS AND DISCUSSION

Equations (10) and (11), together with appropriate boundary conditions, constitute the nonlinear system of equations we shall solve numerically. The numerical calculations to be presented were performed on a two-dimensional cartesian (x,y) mesh using 42 points in the x (east-west) direction, and 142 points in the y (vertical) direction. The (uniform) grid spacing was 2 km in the y direction for all calculations. The grid spacing in the x

direction was 200m in the "small" horizontal scale length cases and 5 km in the "large" cases. The bottom of the grid corresponds to 282 km altitude and the top of the grid to 564 km altitude in all simulations. Periodic boundary conditions were imposed on both n and $\phi_1$ in the x-direction. In the y direction transmittive boundary conditions were imposed on $n(\partial n/\partial y = 0)$ and Neumann $(\partial \phi_1/\partial y = 0)$ boundary conditions were imposed on $\phi_i$.

Three kinds of plots will be presented: (1) contours of constant $n(x,y,t)$; (2) contours of constant $n(x,y,t)/n_o(y,t)$; and (3) contours of constant electrostatic potential $\phi_1$. Superimposed on each contour plot is a dashed line depicting $n_o(y,t)$ for reference purposes. Our initial electron density profile $n_o(y,0)$ is taken from data supplied to us by Tsunoda[7]. It is derived from an off-perpendicular VHF ALTAIR scan taken at 08:04 UT on 17 July 1979. We found it necessary to introduce some smoothing of the raw data using a standard Shuman filter in order to eliminate spurious regions of stability and instability in the initial profile. In general, the bottomside gradient scale lengths associated with this profile are quite a bit larger than those we have used in previous simulations.[4,5] This factor by itself would tend to give us smaller linear growth rates for the collisional Rayleigh-Taylor instability. However, this decrease in linear growth rate is offset by the fact that the whole ionosphere is somewhat higher (this effect tends to increase the linear growth rate) than that used in our previous work (see reference 4 for details). However, the higher altitude of the ionosphere will not offset one other effect of the large initial gradient scale lengths, viz., displacing a plasma fluid element vertically a given distance will result in a smaller relative depletion level. Thus, all other things being equal, larger gradient scale lengths in the initial electron
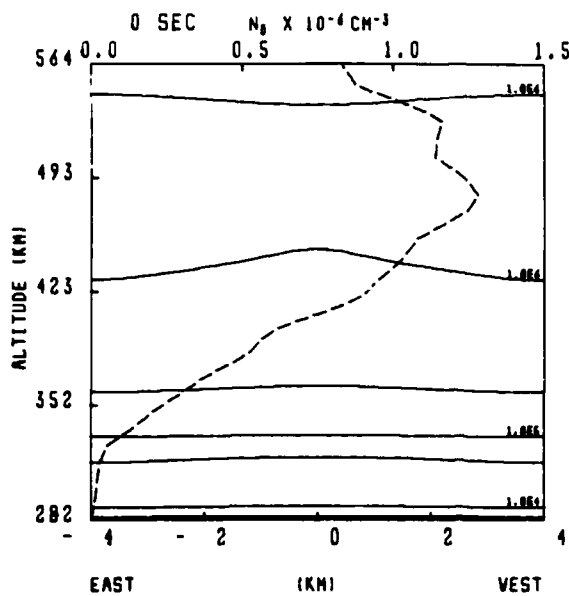
7

density profile will produce less depleted bubbles. To summarize, we expect approximately equal growth times, but less depleted bubbles, than we have seen in our previous work.

Our initial perturbation is given by a pure sine wave of wavelength 40 $\Delta x$ (our system length in the x direction):
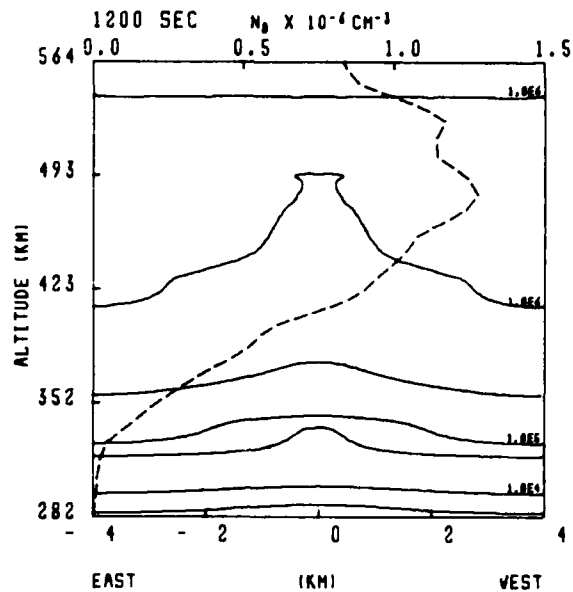
$$\frac{n(x,y,0)}{n_o(y,0)} = 1 - e^{-3} \cos\left(\frac{\pi x}{20\Delta x}\right) \tag{12}$$

Two simulations have been run: i) S, with $\Delta x$ = 200m; and ii) L, with $\Delta x$ = 5 km. These two cases are meant to span the range of actual observed horizontal scale lengths. Figure 2 shows isodensity contours of calculation S at six times during the simulation. Figure 3 shows the same contours at six different times for calculation L. The presence of lower density plasma in the bubble in calculation L is obvious. Also obvious is the fact that calculation S seems to proceed in two separate stages, with a small, low depletion level bubble going through the F2 peak at about 1200 seconds, followed by the main, somewhat more depleted, bubble 800 seconds later. This is in contrast to calculation L where plasma from much lower altitudes is drawn up into the bubble in one stage. Note that in both cases we have fully developed plumes (bubbles) in 2000 seconds.
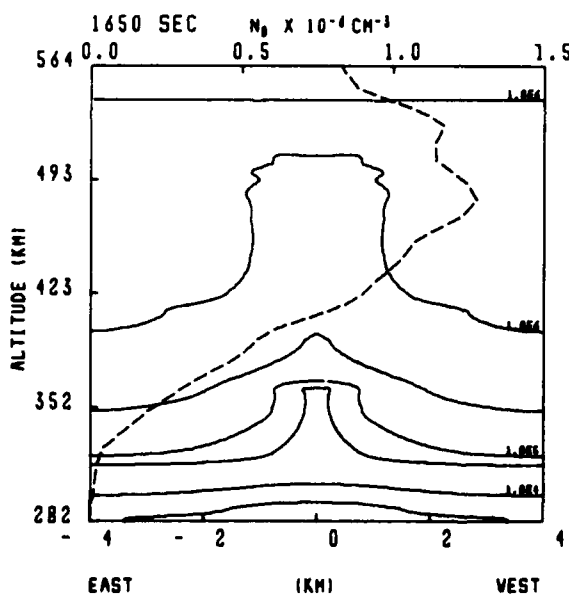
Late time contours of relative electron density $n(x,y,t)/n_o(y,t)$ are shown for calculations S and L in Figures 4a and 4b respectively. Solid lines define depleted regions, while dashed lines define enhancements. For depletions, the contour levels are such that for the first (outermost) contour $n/n_o$ is 0.5, and for each succeeding contour $n/n_o$ is multiplied by 0.5. Thus, the third solid contour line represents a value of $n/n_o$ equal to
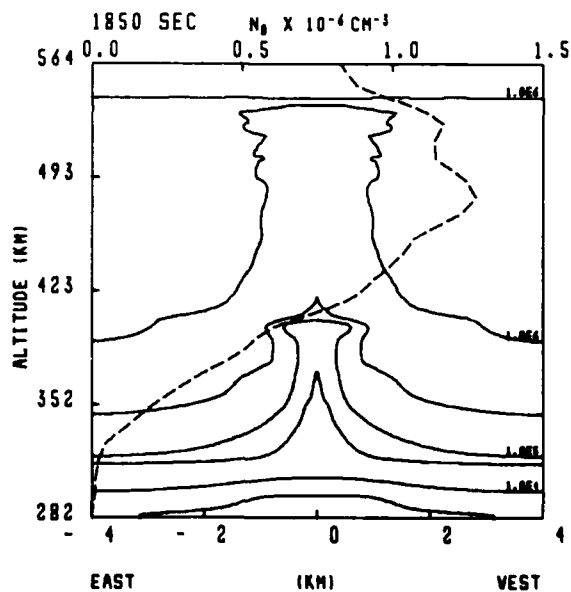
8

0 SEC   $N_e$ X $10^{-4}$ CM$^{-3}$

564 0.0          0.5          1.0          1.5

493

ALTITUDE (KM)

423

1.0E4

352

1.0E5

282

1.0E6

− 4        − 2         0          2          4

EAST              (KM)              VEST

(a)

1200 SEC   $N_e$ X $10^{-4}$ CM$^{-3}$

564 0.0          0.5          1.0          1.5

493

ALTITUDE (KM)

423

1.0E4

352

1.0E5

282

1.0E6

− 4        − 2         0          2          4

EAST              (KM)              VEST

(b)

1650 SEC   $N_e$ X $10^{-4}$ CM$^{-3}$

564 0.0          0.5          1.0          1.5

493

ALTITUDE (KM)

423

1.0E4

352

1.0E5

282

1.0E6

− 4        − 2         0          2          4

EAST              (KM)              VEST

(c)

1850 SEC   $N_e$ X $10^{-4}$ CM$^{-3}$

564 0.0          0.5          1.0          1.5

493

ALTITUDE (KM)

423

1.0E4

352

1.0E5

282

1.0E6

− 4        − 2         0          2          4

EAST              (KM)              VEST

(d)

Fig. 2 — Sequence of six plots showing iso-electron density contours of calculation S at 0, 1200, 1650, 1850, 1950, and 2050 sec. Superimposed on each plot is a long dashed line depicting $n_o(y,t)$. Electron densities are given in cm$^{-3}$. The observer is looking southward.
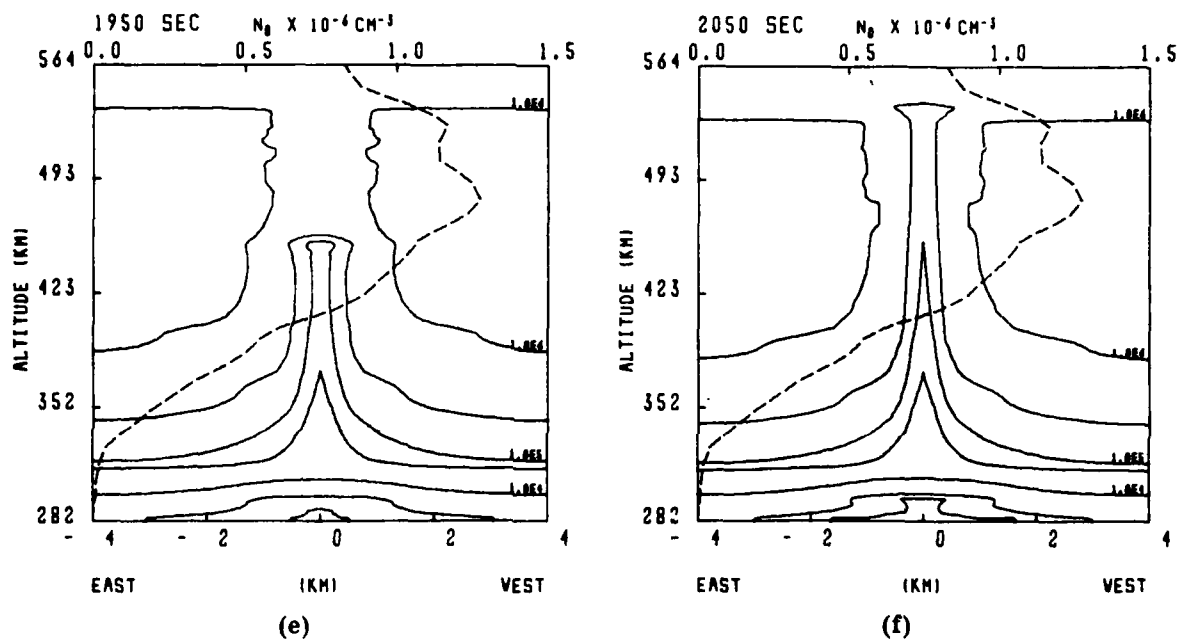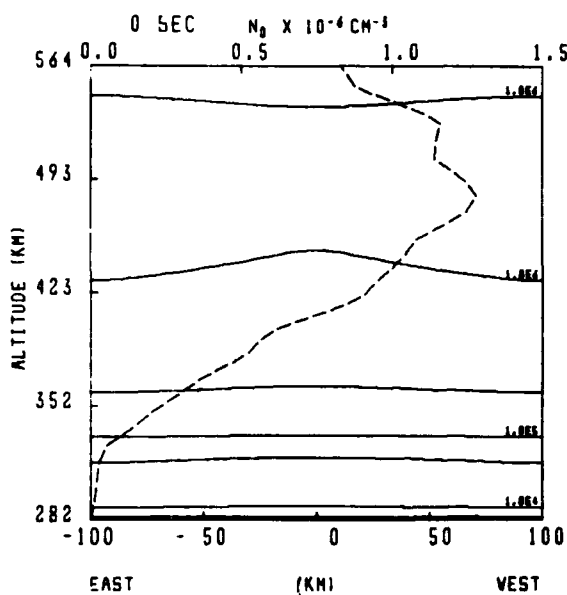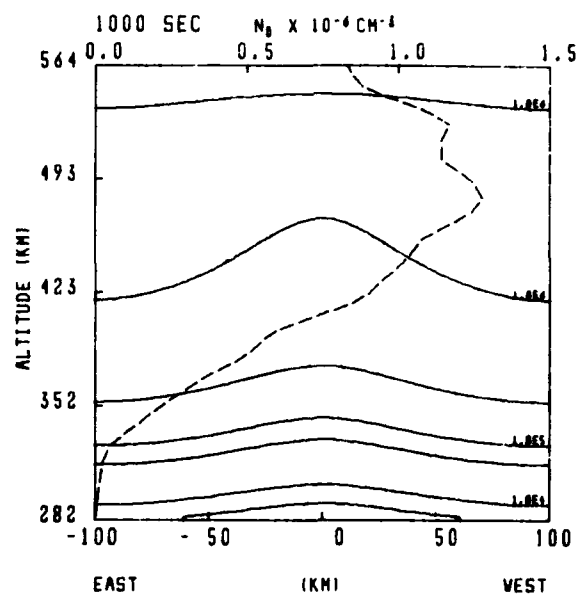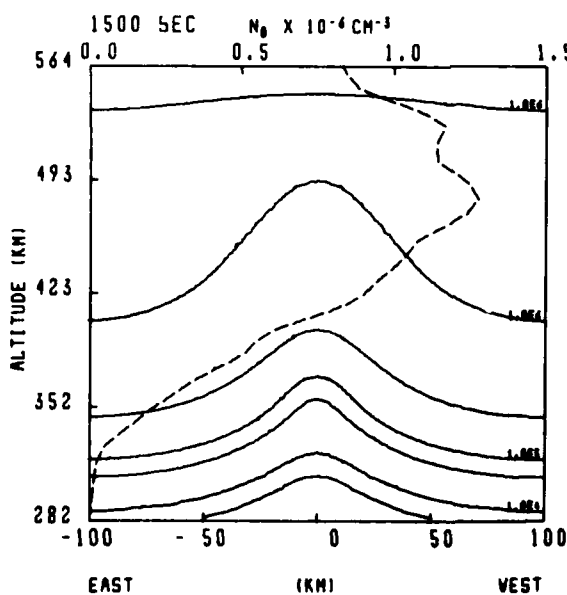
9

Fig. 2(Cont'd) — Sequence of six plots showing iso-electron density contours of calculation S at 0, 1200, 1650, 1850, 1950, and 2050 sec. Superimposed on each plot is a long dashed line depicting $n_o(y,t)$. Electron densities are given in $cm^{-3}$. The observer is looking southward.
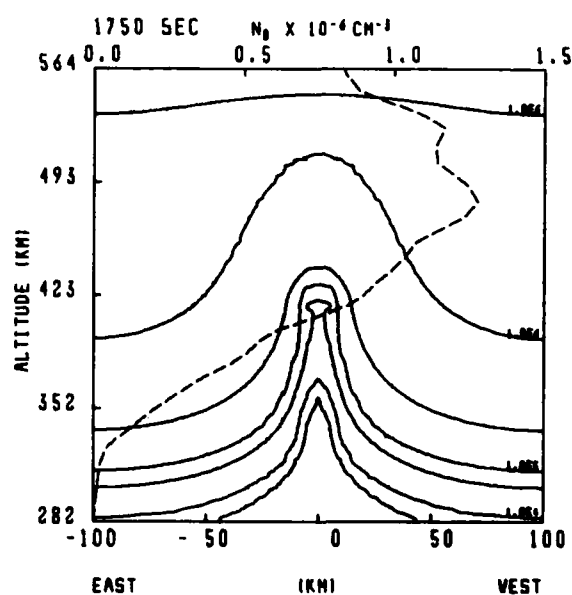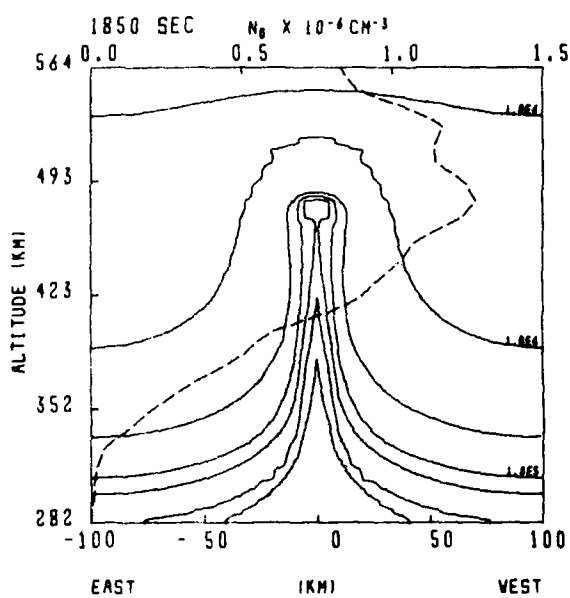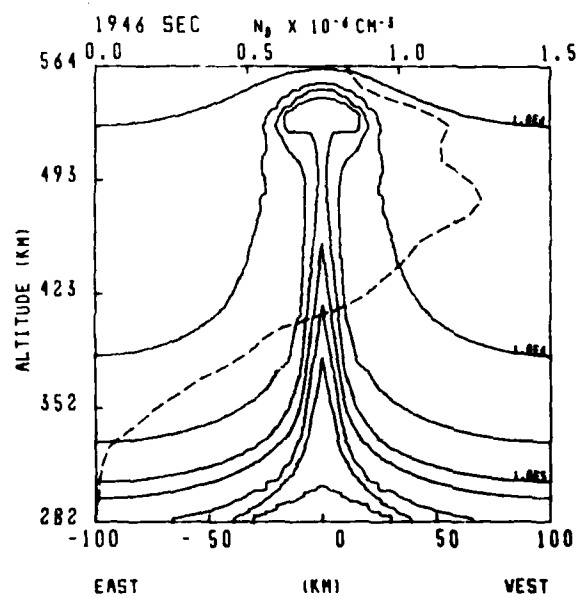
Fig. 3 — Sequence of six plots showing iso-electron density contours of calculation L at 0, 1000, 1500, 1750, 1850, and 1946 sec. Superimposed on each plot is a long dashed line depicting $n_o(y,t)$. Electron densities are given in $cm^{-3}$. The observer is looking southward.

11

Fig. 3(Cont'd) — Sequence of six plots showing iso-electron density contours of calculation L at 0, 1000, 1500, 1750, 1850, and 1946 sec. Superimposed on each plot is a long dashed line depicting $n_o(y,t)$. Electron densities are given in $cm^{-3}$. The observer is looking southward.
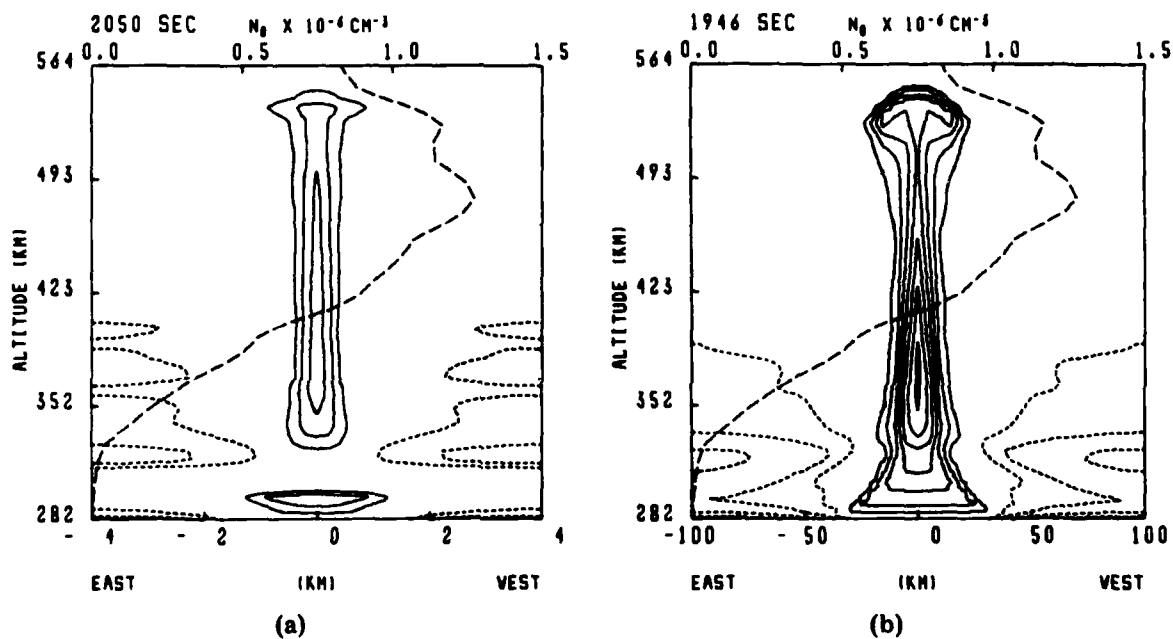
Fig. 4 — Contours of constant $n(x,y,t)/n_0(y,t)$ for a) calculation S at 2050 sec and b) calculation L at 1946 sec. Depletions ($n/n_0 < 1$) are shown as solid lines while enhancements ($n/n_0 > 1$) are shown as short dashed lines. The first (outermost) depletion contour is for $n/n_0 = 0.5$, while each succeeding contour is for a value of $n/n_0$ a factor of 0.5 times the previous one. The first enhancement contour is for $n/n_0 = 2.0$, while each succeeding contour is for a value of $n/n_0$ a factor of 2.0 times the previous one. The superimposed long dashed line depicts $n_0(y,t)$.

13

$(0.5)^3 = 0.125$, or an 87.5% depletion. For the first dashed contour line, $n/n_o$ is 2.0, and for each succeeding contour line $n/n_o$ is multiplied by 2.0. Percentage enhancements and depletions are obtained by subtracting 1.0 from $n/n_o$. Comparison of figures 4a and 4b shows that the depletion level of the large horizontal scale bubble is greater than that of the small horizontal scale bubble. Furthermore, neither of these calculations attain the depletion levels seen in our previous work (see Figure 7 in reference 5). For instance, in the calculation shown in Figure 7b of reference 5, which is identical to our calculation L except for the initial ambient electron density profile, a plume of almost 200 km vertical extent can be found with depletion levels of 99.9% or greater. A look at Figure 4b shows that a plume of similar dimensions can be found only for depletion levels of 94% or greater. These smaller depletion levels for the ALTAIR profile were expected based on our analysis of the effects of larger gradient scale lengths in the initial electron density profile, presented earlier in this section. An explanation of why larger horizontal scale lengths produce more severely depleted bubbles is given in reference 5. Briefly, scale analysis is invoked to show that the vertical extent of the polarization electric field produced by a perturbation in the ionosphere scales as the horizontal extent of that perturbation. Since it is the electric field which produces plasma movement, the vertical extent of the polarization electric field will determine the depth in the ionosphere from which a bubble may draw plasma. The lower in altitude that a plasma fluid element originates, the lower its density and hence the higher the depletion level of any plume into which it is drawn (see reference 5 for details). To illustrate this point, we show in Figures 5a and 5b contours of the polarization potential $\phi_1$, for calculation S at 1650 seconds and for
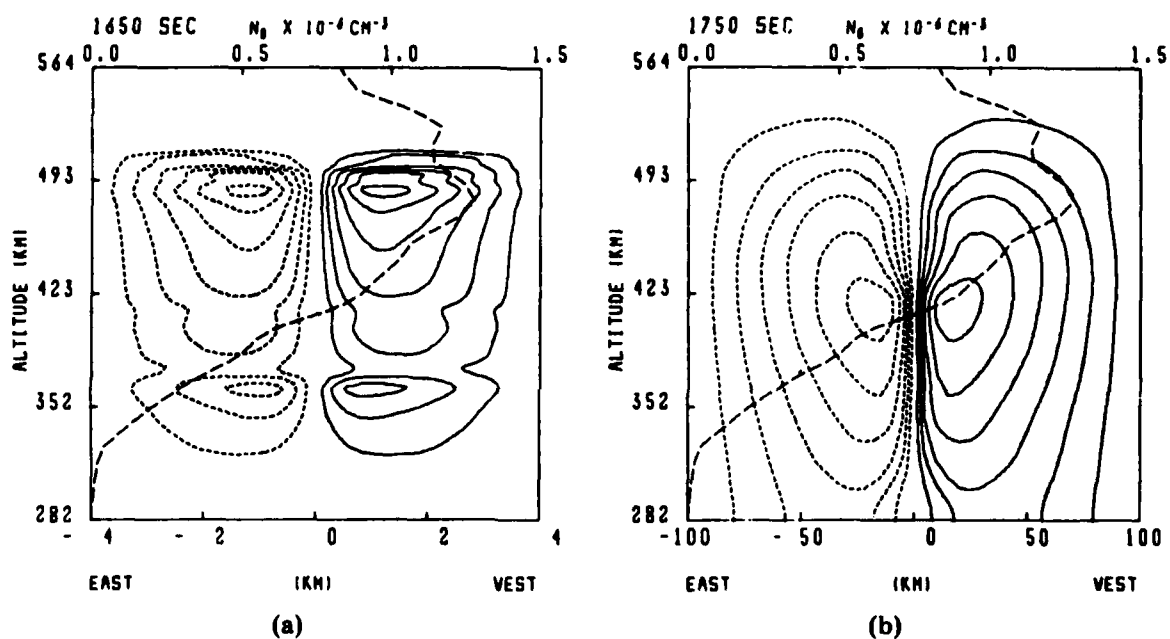
14

Fig. 5 — Contours of constant electrostatic potential $\phi_1$ for a) calculation S at 1650 sec. and b) calculation L at 1750 sec. Positive potentials are shown as solid lines, while negative potentials are shown as short dashed lines. The contour levels are equally spaced from minimum to maximum, except that the zero contour is suppressed. Superimposed on each plot is a long dashed line depicting $n_o(y,t)$.

calculation L at 1750 seconds, respectively. Contours of constant $\phi_1$ are in fact streamlines for this flow (see (4) and (6)). Calculation S is seen to consist of two convective cells, each mixing plasma over a fairly narrow altitude range, while calculation L has formed a deep convective cell, drawing plasma into the plume from very low altitudes.

## IV. SUMMARY

Both of our global large scale collisional Rayleigh-Taylor nonlinear simulations, using a background electron density profile from ALTAIR incoherent radar measurements on 17 July 1979 prior to spread F onset, indicate fully developed ESF bubbles in approximately one-half hour. ALTAIR radar and ionosonde measurements indicate fully developed spread F backscatter about one hour after the profile was taken. The most obvious explanation is that perhaps we have simply chosen our perturbation amplitude too large; however, since no in situ measurements were made prior to ESF the measurements do not provide us with all the pertinent initial conditions prior to ESF onset. Other factors such as the shorting effects of background E region conductivities or the neglect of inertial terms in the ion momentum equation could also influence the speed with which the instability proceeds. In addition, since the chain of events which leads from kilometer scale bubbles to one meter backscatter irregularities is not well understood, neither are the associated time delays. Nevertheless, our simulations exhibit results which are con-sistent with the onset time of ESF during the 17 July 1979 Kwajalein campaign.

A word of caution is in order here with regard to a comparison of the bubbles we show in our simulations and the actual structures into which the PLUMEX I rocket was launched[8,9] at 12:31 UT on 17 July 1979. According to ALTAIR measurements[6], starting with the onset of spread F at about 09:00 UT

and lasting until approximately the time of rocket launch, the bottomside of the F region moved downward approximately 140 km at the same time developing much smaller gradient scale lengths[9] than we have used in the present simulation. In addition, the bubbles detected by the in situ plasma probe at these later times shows depletions $\lesssim$ 90%. At least three factors are in competition here: 1) the downward movement of the ionospheric plasma indicates the presence of an electric field which would tend to reduce the growth rate of the instability; 2) lower altitudes mean larger $\nu_{in}$ which again would reduce the growth rate; and 3) the development of smaller bottomside gradient scale lengths would enhance the growth rate. In addition, the ALTAIR radar operating in the coherent mode showed that VHF plumes (looking at 1m field aligned irregularities) at this late time during ESF were in a decay phase of development. Decaying plumes which had been generated early while the iono- sphere was high would not disappear simply because the plasma had been dis- placed downward later in the evening. Obviously the actual physical situation at the rocket launch time is more complex than that addressed by the simulations presented here, although many of these complexities will be treated accurately in forthcoming versions of our simulation model.

### Acknowledgments

## REFERENCES

1. B. B. Balsley, G. Haerendel and R. A. Greenwald, "Equatorial Spread F: Recent Observations and a New Interpretation," _J. Geophys. Res._, 77, 5625, 1972.

2. G. Haerendel, "Theory of Equatorial Spread F," report, Max-Planck Inst. fur Phys. and Astrophys., Garching, West Germany, 1974.

3. A. J. Scannapieco and S. L. Ossakow, "Nonlinear Equatorial Spread F," _Geophys. Res. Lett._, 3, 451, 1976.

4. S. L. Ossakow, S. T. Zalesak, B. E. McDonald, and P. K. Chaturvedi, "Nonlinear Equatorial Spread F: Dependence on Altitude of F Peak and Bottomside Background Electron Density Gradient Scale Length," _J. Geophys. Res._, 84, 17, 1979.

5. S. T. Zalesak, and S. L. Ossakow, "Nonlinear Equatorial Spread F: Spatially Large Bubbles Resulting from Large Horizontal Scale Initial Perturbations," _J. Geophys. Res._, 85, 2131, 1980.

6. R. T. Tsunoda, "ALTAIR Radar Measurements in Support of the PLUMEX Rocket Campaign," DNA Report (in press).

7. R. T. Tsunoda, _private communication_, 1980.

8. E. P. Szuszczewicz, R. T. Tsunoda, R. Narcisi, and J. C. Holmes, "PLUMEX I: Coincident Radar and Rocket Observations of Equatorial Spread F," NRL Memo Report 4201, March 1980.

9. E. P. Szuszczewicz, and J. C. Holmes, "Equatorial Spread F: 'In Situ' Measurements of Electron Density, Temperature and Density Fluctuation Power Spectra," NRL Memo Report 4289, August 1980.

# DISTRIBUTION LIST

DEPARTMENT OF DEFENSE

ASSISTANT SECRETARY OF DEFENSE
COMM, CMD, CONT & INTELL
WASHINGTON, D.C. 20301
    01CY ATTN J. BABCOCK
    01CY ATTN M. EPSTEIN

ASSISTANT TO THE SECRETARY OF DEFENSE
ATOMIC ENERGY
WASHINGTON, D.C. 20301
    01CY ATTN EXECUTIVE ASSISTANT

DIRECTOR
COMMAND CONTROL TECHNICAL CENTER
PENTAGON RM BE 685
WASHINGTON, D.C. 20301
    01CY ATTN C-650
    01CY ATTN C-312 R. MASON

DIRECTOR
DEFENSE ADVANCED RSCH PROJ AGENCY
ARCHITECT BUILDING
1400 WILSON BLVD.
ARLINGTON, VA. 22209
    01CY ATTN NUCLEAR MONITORING RESEARCH
    01CY ATTN STRATEGIC TECH OFFICE

DEFENSE COMMUNICATION ENGINEER CENTER
1860 WIEHLE AVENUE
RESTON, VA. 22090
    01CY ATTN CODE R820
    01CY ATTN CODE R410 JAMES W. MCLEAN
    01CY ATTN CODE R720 J. WORTHINGTON

DIRECTOR
DEFENSE COMMUNICATIONS AGENCY
WASHINGTON, D.C. 20305
    (ADR CNWDI: ATTN CODE 240 FOR)
    01CY ATTN CODE 101B

DEFENSE TECHNICAL INFORMATION CENTER
CAMERON STATION
ALEXANDRIA, VA. 22314
    (12 COPIES IF OPEN PUBLICATION, OTHERWISE 2 COPIES)
    12CY ATTN TC

DIRECTOR
DEFENSE INTELLIGENCE AGENCY
WASHINGTON, D.C. 20301
    01CY ATTN DT-1B
    01CY ATTN DB-4C E. O'FARRELL
    01CY ATTN DIAAP A. WISE
    01CY ATTN DIAST-5
    01CY ATTN DT-1BZ R. MORTON
    01CY ATTN HQ-TR J. STEWART
    01CY ATTN W. WITTIG DC-7D

DIRECTOR
DEFENSE NUCLEAR AGENCY
WASHINGTON, D.C. 20305
    01CY ATTN STVL
    04CY ATTN TITL
    01CY ATTN DDST
    03CY ATTN RAAE

COMMANDER
FIELD COMMAND
DEFENSE NUCLEAR AGENCY
KIRTLAND AFB, NM 87115
    01CY ATTN FCPR

DIRECTOR
INTERSERVICE NUCLEAR WEAPONS SCHOOL
KIRTLAND AFB, NM 87115
    01CY ATTN DOCUMENT CONTROL

JOINT CHIEFS OF STAFF
WASHINGTON, D.C. 20301
    01CY ATTN J-3 WWMCCS EVALUATION OFFICE

DIRECTOR
JOINT STRAT TGT PLANNING STAFF
OFFUTT AFB
OMAHA, NB 68113
    01CY ATTN JLTW-2
    01CY ATTN JPST G. GOETZ

CHIEF
LIVERMORE DIVISION FLD COMMAND DNA
DEPARTMENT OF DEFENSE
LAWRENCE LIVERMORE LABORATORY
P. O. BOX 808
LIVERMORE, CA 94550
    01CY ATTN FCPRL

DIRECTOR
NATIONAL SECURITY AGENCY
DEPARTMENT OF DEFENSE
FT. GEORGE G. MEADE, MD 20755
    01CY ATTN JOHN SKILLMAN R52
    01CY ATTN FRANK LEONARD
    01CY ATTN W14 PAT CLARK
    01CY ATTN OLIVER H. BARTLETT W32
    01CY ATTN R5

COMMANDANT
NATO SCHOOL (SHAPE)
APO NEW YORK 09172
    01CY ATTN U.S. DOCUMENTS OFFICER

UNDER SECY OF DEF FOR RSCH & ENGRG
DEPARTMENT OF DEFENSE
WASHINGTON, D.C. 20301
    01CY ATTN STRATEGIC & SPACE SYSTEMS (OS)

WWMCCS SYSTEM ENGINEERING ORG
WASHINGTON, D.C. 20305
    01CY ATTN R. CRAWFORD

COMMANDER/DIRECTOR
ATMOSPHERIC SCIENCES LABORATORY
U.S. ARMY ELECTRONICS COMMAND
WHITE SANDS MISSILE RANGE, NM 88002
    01CY ATTN DELAS-EO F. NILES

DIRECTOR
BMD ADVANCED TECH CTR
HUNTSVILLE OFFICE
P. O. BOX 1500
HUNTSVILLE, AL 35807
    01CY ATTN ATC-T MELVIN T. CAPPS
    01CY ATTN ATC-O W. DAVIES
    01CY ATTN ATC-R DON RUSS

PROGRAM MANAGER
BMD PROGRAM OFFICE
5001 EISENHOWER AVENUE
ALEXANDRIA, VA 22333
    01CY ATTN DACS-BMT J. SHEA

CHIEF C-E SERVICES DIVISION
U.S. ARMY COMMUNICATIONS CMD
PENTAGON RM 1B269
WASHINGTON, D.C. 20310
    01CY ATTN C-E-SERVICES DIVISION

COMMANDER
FRADCOM TECHNICAL SUPPORT ACTIVITY
DEPARTMENT OF THE ARMY
FORT MONMOUTH, N.J. 07703
    01CY ATTN DRSEL-NL-RD H. BENNET
    01CY ATTN DRSEL-PL-ENV H. BOMKE
    01CY ATTN J. E. QUIGLEY

COMMANDER
HARRY DIAMOND LABORATORIES
DEPARTMENT OF THE ARMY
2800 POWDER MILL ROAD
ADELPHI, MD 20783
        (CNWDI-INNER ENVELOPE: ATTN: DELHD-RBH)
    01CY  ATTN DELHD-TI  M. WEINER
    01CY  ATTN DELHD-RB  R. WILLIAMS
    01CY  ATTN DELHD-NP  F. WIMENITZ
    01CY  ATTN DELHD-NP  C. MOAZED


COMMANDER
U.S. ARMY COMM-ELEC ENGRG INSTAL AGY
FT. HUACHUCA, AZ  85613

    01CY  ATTN CCC-EMEO  GEORGE LANE


COMMANDER
U.S. ARMY FOREIGN SCIENCE & TECH CTR
220 7TH STREET, NE
CHARLOTTESVILLE, VA  22901
    01CY  ATTN DRXST-SD
    01CY  ATTN R. JONES


COMMANDER
U.S. ARMY MATERIEL DEV & READINESS CMD
5001 EISENHOWER AVENUE
ALEXANDRIA, VA  22333
    01CY  ATTN DRCLDC  J. A. BENDER


COMMANDER
U.S. ARMY NUCLEAR AND CHEMICAL AGENCY
7500 BACKLICK ROAD
BLDG 2073
SPRINGFIELD, VA  22150
    01CY  ATTN LIBRARY

DIRECTOR
U.S. ARMY BALLISTIC RESEARCH LABS
ABERDEEN PROVING GROUND, MD  21005
    01CY  ATTN TECH LIB  EDWARD BAICY

COMMANDER
U.S. ARMY SATCOM AGENCY
FT. MONMOUTH, NJ  07703
    01CY  ATTN DOCUMENT CONTROL


COMMANDER
U.S. ARMY MISSILE INTELLIGENCE AGENCY
REDSTONE ARSENAL, AL  35809
    01CY  ATTN JIM GAMBLE


DIRECTOR
U.S. ARMY TRADOC SYSTEMS ANALYSIS ACTIVITY
WHITE SANDS MISSILE RANGE, NM  88002
    01CY  ATTN ATAA-SA
    01CY  ATTN TCC/F. PAYAN JR.
    01CY  ATTN ATAA-TAC LTC J. HESSE

COMMANDER
NAVAL ELECTRONIC SYSTEMS COMMAND
WASHINGTON, D.C.  20360
    01CY  ATTN NAVALEX 034 T. HUGHES
    01CY  ATTN PME 117
    01CY  ATTN PME 117-T
    01CY  ATTN CODE 5011

COMMANDING OFFICER
NAVAL INTELLIGENCE SUPPORT CTR
4301 SUITLAND ROAD, BLDG. 5
WASHINGTON, D.C.  20390
    01CY  ATTN MR. DUBBIN  STIC 12
    01CY  ATTN NISC-50
    01CY  ATTN CODE 5404 J. GALET


COMMANDER
NAVAL OCEAN SYSTEMS CENTER
SAN DIEGO, CA  92152
    03CY  ATTN CODE 532  W. MOLER
    01CY  ATTN CODE 0230  C. BAGGETT
    01CY  ATTN CODE 81  R. EASTMAN


DIRECTOR
NAVAL RESEARCH LABORATORY
WASHINGTON, D.C.  20375
    01CY  ATTN CODE 4700  T. P. COFFEY (25 CYS IF UN, 1 CY IF CLASS)
    01CY  ATTN CODE 4701  JACK D. BROWN
    01CY  ATTN CODE 4780  BRANCH HEAD (150 CYS IF UN, 1 CY IF CLASS)
    01CY  ATTN CODE 7500  HQ COMM DIR  BRUCE WALD
    01CY  ATTN CODE 7550  J. DAVIS
    01CY  ATTN CODE 7580
    01CY  ATTN CODE 7551
    01CY  ATTN CODE 7555
    01CY  ATTN CODE 4730  E. MCLEAN
    01CY  ATTN CODE 4127  C. JOHNSON

COMMANDER
NAVAL SEA SYSTEMS COMMAND
WASHINGTON, D.C.  20362
    01CY  ATTN  CAPT R. PITKIN

COMMANDER
NAVAL SPACE SURVEILLANCE SYSTEM
DAHLGREN, VA  22448
    01CY  ATTN CAPT J. H. BURTON

OFFICER-IN-CHARGE
NAVAL SURFACE WEAPONS CENTER
WHITE OAK, SILVER SPRING, MD  20910
    01CY  ATTN CODE F31


DIRECTOR
STRATEGIC SYSTEMS PROJECT OFFICE
DEPARTMENT OF THE NAVY
WASHINGTON, D.C.  20376
    01CY  ATTN NSP-2141
    01CY  ATTN NSSP-2722  FRED WIMBERLY

NAVAL SPACE SYSTEM ACTIVITY
P. O. BOX 92960
WORLDWAY POSTAL CENTER
LOS ANGELES, CALIF.  90009
    01CY  ATTN  A. B. HAZZARD


COMMANDER
NAVAL SURFACE WEAPONS CENTER
DAHLGREN LABORATORY
DAHLGREN, VA  22448
    01CY  ATTN CODE DF-14  R. BUTLER


COMMANDING OFFICER
NAVY SPACE SYSTEMS ACTIVITY
P.O. BOX 92960
WORLDWAY POSTAL CENTER
LOS ANGELES, CA.  90009
    01CY  ATTN CODE 52

OFFICE OF NAVAL RESEARCH
ARLINGTON, VA  22217
    01CY  ATTN CODE 465
    01CY  ATTN CODE 461
    01CY  ATTN CODE 402
    01CY  ATTN CODE 420
    01CY  ATTN CODE 421

COMMANDER
AEROSPACE DEFENSE COMMAND/DC
DEPARTMENT OF THE AIR FORCE
ENT AFB, CO  80912
    01CY  ATTN DC  MR. LONG

COMMANDER
AEROSPACE DEFENSE COMMAND/XPO
DEPARTMENT OF THE AIR FORCE
ENT AFB, CO  80912
    01CY  ATTN XPDQQ
    01CY  ATTN XP

AIR FORCE GEOPHYSICS LABORATORY
HANSCOM AFB, MA  01731
    01CY  ATTN OPR  HAROLD GARDNER
    01CY  ATTN OPR-1 JAMES C. ULWICK
    01CY  ATTN LKB  KENNETH S. W. CHAMPION
    01CY  ATTN OPR  ALVA T. STAIR
    01CY  ATTN PHP  JULES AARONS
    01CY  ATTN PHD  JURGEN BUCHAU
    01CY  ATTN PHD  JOHN P. MULLEN

AF WEAPONS LABORATORY
KIRTLAND AFB, NM  87117
 01CY ATTN SUL
 01CY ATTN CA ARTHUR H. GUENTHER
 01CY ATTN DYC CAPT J. BARRY
 01CY ATTN DYC JOHN M. KAMM
 01CY ATTN DYT CAPT MARK A. FRY
 01CY ATTN DES MAJ GARY GANONG
 01CY ATTN DYC J. JANNI

AFTAC
PATRICK AFB, FL  32925
 01CY ATTN TF/MAJ WILEY
 01CY ATTN TN

AIR FORCE AVIONICS LABORATORY
WRIGHT-PATTERSON AFB, OH  45433
 01CY ATTN AAD WADE HUNT
 01CY ATTN AAD ALLEN JOHNSON

DEPUTY CHIEF OF STAFF
RESEARCH, DEVELOPMENT, & ACQ
DEPARTMENT OF THE AIR FORCE
WASHINGTON, D.C.  20330
 01CY ATTN AFRDQ

HEADQUARTERS
ELECTRONIC SYSTEMS DIVISION/XR
DEPARTMENT OF THE AIR FORCE
HANSCOM AFB, MA  01731
 01CY ATTN XR J. DEAS

HEADQUARTERS
ELECTRONIC SYSTEMS DIVISION/YSEA
DEPARTMENT OF THE AIR FORCE
HANSCOM AFB, MA  01731
 01CY ATTN YSEA

HEADQUARTERS
ELECTRONIC SYSTEMS DIVISION/DC
DEPARTMENT OF THE AIR FORCE
HANSCOM AFB, MA  01731
 01CY ATTN DCKC MAJ J.C. CLARK

COMMANDER
FOREIGN TECHNOLOGY DIVISION, AFSC
WRIGHT-PATTERSON AFB, OH  45433
 01CY ATTN NICD LIBRARY
 01CY ATTN ETDP B. BALLARD

COMMANDER
ROME AIR DEVELOPMENT CENTER, AFSC
GRIFFISS AFB, NY  13441
 01CY ATTN DOC LIBRARY/TSLD
 01CY ATTN OCSE V. COYNE

SAMSO/SZ
POST OFFICE BOX 92960
WORLDWAY POSTAL CENTER
LOS ANGELES, CA  90009
(SPACE DEFENSE SYSTEMS)
 01CY ATTN SZJ

STRATEGIC AIR COMMAND/XPFS
OFFUTT AFB, NB  68113
 01CY ATTN XPFS MAJ B. STEPHAN
 01CY ATTN ADWATE MAJ BRUCE BAUER
 01CY ATTN NRT
 01CY ATTN DOK CHIEF SCIENTIST

SAMSO/SK
P. O. BOX 92960
WORLDWAY POSTAL CENTER
LOS ANGELES, CA  90009
 01CY ATTN SKA (SPACE COMM SYSTEMS) M. CLAVIN

SAMSO/MN
NORTON AFB, CA  92409
(MINUTEMAN)
 01CY ATTN MNNL LTC KENNEDY

COMMANDER
ROME AIR DEVELOPMENT CENTER, AFSC
HANSCOM AFB, MA  01731
 01CY ATTN EEP A. LORENTZEN

DEPARTMENT OF ENERGY
ALBUQUERQUE OPERATIONS OFFICE
P. O. BOX 5400
ALBUQUERQUE, NM  87115
 01CY ATTN DOC CON FOR D. SHERWOOD

DEPARTMENT OF ENERGY
LIBRARY ROOM G-042
WASHINGTON, D.C.  20545
 01CY ATTN DOC CON FOR A. LABOWITZ

EG&G, INC.
LOS ALAMOS DIVISION
P. O. BOX 809
LOS ALAMOS, NM  85544
 01CY ATTN DOC CON FOR J. BREEDLOVE

UNIVERSITY OF CALIFORNIA
LAWRENCE LIVERMORE LABORATORY
P. O. BOX 808
LIVERMORE, CA  94550
 01CY ATTN DOC CON FOR TECH INFO DEPT
 01CY ATTN DOC CON FOR L-389 R. OTT
 01CY ATTN DOC CON FOR L-31 R. HAGER
 01CY ATTN DOC CON FOR L-46 F. SEWARD

LOS ALAMOS SCIENTIFIC LABORATORY
P. O. BOX 1663
LOS ALAMOS, NM  87545
 01CY ATTN DOC CON FOR J. WOLCOTT
 01CY ATTN DOC CON FOR R. F. TASCHEK
 01CY ATTN DOC CON FOR E. JONES
 01CY ATTN DOC CON FOR J. MALIK
 01CY ATTN DOC CON FOR R. JEFFRIES
 01CY ATTN DOC CON FOR J. ZINN
 01CY ATTN DOC CON FOR P. KEATON
 01CY ATTN DOC CON FOR D. WESTERVELT

SANDIA LABORATORIES
P. O. BOX 5800
ALBUQUERQUE, NM  87115
 01CY ATTN DOC CON FOR J. MARTIN
 01CY ATTN DOC CON FOR W. BROWN
 01CY ATTN DOC CON FOR A. THORNBROUGH
 01CY ATTN DOC CON FOR T. WRIGHT
 01CY ATTN DOC CON FOR D. DAHLGREN
 01CY ATTN DOC CON FOR 3141
 01CY ATTN DOC CON FOR SPACE PROJECT DIV

SANDIA LABORATORIES
LIVERMORE LABORATORY
P. O. BOX 969
LIVERMORE, CA  94550
 01CY ATTN DOC CON FOR B. MURPHEY
 01CY ATTN DOC CON FOR T. COOK

OFFICE OF MILITARY APPLICATION
DEPARTMENT OF ENERGY
WASHINGTON, D.C.  20545
 01CY ATTN DOC CON FOR D. GALE

OTHER GOVERNMENT

CENTRAL INTELLIGENCE AGENCY
ATTN RD/SI, RM 5G48, HQ BLDG
WASHINGTON, D.C.  20505
 01CY ATTN OSI/PSID RM 5F 19

DEPARTMENT OF COMMERCE
NATIONAL BUREAU OF STANDARDS
WASHINGTON, D.C.  20234
 (ALL CORRES:  ATTN SEC OFFICER FOR)
 01CY ATTN R. MOORE

INSTITUTE FOR TELECOM SCIENCES
NATIONAL TELECOMMUNICATIONS & INFO ADMIN
BOULDER, CO 80303
    01CY  ATTN A. JEAN (UNCLASS ONLY)
    01CY  ATTN W. UTLAUT
    01CY  ATTN D. CROMBIE
    01CY  ATTN L. BERRY

NATIONAL OCEANIC & ATMOSPHERIC ADMIN
ENVIRONMENTAL RESEARCH LABORATORIES
DEPARTMENT OF COMMERCE
BOULDER, CO 80302
    01CY  ATTN R. GRUBB
    01CY  ATTN AERONOMY LAB  G. REID

DEPARTMENT OF DEFENSE CONTRACTORS

AEROSPACE CORPORATION
P. O. BOX 92957
LOS ANGELES, CA 90009
    01CY  ATTN I. GARFUNKEL
    01CY  ATTN T. SALMI
    01CY  ATTN V. JOSEPHSON
    01CY  ATTN S. BOWER
    01CY  ATTN N. STOCKWELL
    01CY  ATTN D. OLSEN

    01CY  ATTN SMFA FOR PWW

ANALYTICAL SYSTEMS ENGINEERING CORP
5 OLD CONCORD ROAD
BURLINGTON, MA 01803
    01CY  ATTN RADIO SCIENCES

BERKELEY RESEARCH ASSOCIATES, INC.
P. O. BOX 983
BERKELEY, CA 94701
    01CY  ATTN J. WORKMAN

BOEING COMPANY, THE
P. O. BOX 3707
SEATTLE, WA 98124
    01CY  ATTN G. KEISTER
    01CY  ATTN D. MURRAY
    01CY  ATTN G. HALL
    01CY  ATTN J. KENNEY

CALIFORNIA AT SAN DIEGO, UNIV OF
P.O. Box 6049
San Diego, CA 92106
    01CY Attn Henry G. Booker

BROWN ENGINEERING COMPANY, INC.
CUMMINGS RESEARCH PARK
HUNTSVILLE, AL 35807
    01CY  ATTN ROMEO A. DELIBERIS

CHARLES STARK DRAPER LABORATORY, INC.
555 TECHNOLOGY SQUARE
CAMBRIDGE, MA 02139
    01CY  ATTN D. B. COX
    01CY  ATTN J. P. GILMORE

COMPUTER SCIENCES CORPORATION
6565 ARLINGTON BLVD
FALLS CHURCH, VA 22046
    01CY  ATTN H. BLANK
    01CY  ATTN JOHN SPOOR
    01CY  ATTN C. NAIL

COMSAT LABORATORIES
LINTHICUM ROAD
CLARKSBURG, MD 20734
    01CY  ATTN G. HYDE

CORNELL UNIVERSITY
DEPARTMENT OF ELECTRICAL ENGINEERING
ITHACA, NY 14850
    01CY  ATTN D. T. FARLEY JR

ELECTROSPACE SYSTEMS, INC.
BOX 1359
RICHARDSON, TX 75080
    01CY  ATTN H. LOGSTON
    01CY  ATTN SECURITY (PAUL PHILLIPS)

ESL INC.
495 JAVA DRIVE
SUNNYVALE, CA 94086
    01CY  ATTN J. ROBERTS
    01CY  ATTN JAMES MARSHALL
    01CY  ATTN C. W. PRETTIE

FORD AEROSPACE & COMMUNICATIONS CORP
3939 FABIAN WAY
PALO ALTO, CA 94303
    01CY  ATTN J. T. MATTINGLEY

GENERAL ELECTRIC COMPANY
SPACE DIVISION
VALLEY FORGE SPACE CENTER
GODDARD BLVD KING OF PRUSSIA
P. O. BOX 8555
PHILADELPHIA, PA 19101
    01CY  ATTN M. H. BORTNER  SPACE SCI LAB

GENERAL ELECTRIC COMPANY
P. O. BOX 1122
SYRACUSE, NY 13201
    01CY  ATTN F. REIBERT

GENERAL ELECTRIC COMPANY
TEMPO-CENTER FOR ADVANCED STUDIES
816 STATE STREET (P.O. DRAWER QQ)
SANTA BARBARA, CA 93102
    01CY  ATTN DASIAC
    01CY  ATTN DON CHANDLER
    01CY  ATTN TOM BARRETT
    01CY  ATTN TIM STEPHANS
    01CY  ATTN WARREN S. KNAPP
    01CY  ATTN WILLIAM MCNAMARA
    01CY  ATTN B. GAMBILL
    01CY  ATTN MACK STANTON

GENERAL ELECTRIC TECH SERVICES CO., INC.
HMES
COURT STREET
SYRACUSE, NY 13201
    01CY  ATTN G. MILLMAN

GENERAL RESEARCH CORPORATION
SANTA BARBARA DIVISION
P. O. BOX 6770
SANTA BARBARA, CA 93111
    01CY  ATTN JOHN ISE JR
    01CY  ATTN JOEL GARBARINO

GEOPHYSICAL INSTITUTE
UNIVERSITY OF ALASKA
FAIRBANKS, AK 99701
        (ALL CLASS ATTN:  SECURITY OFFICER)
    01CY  ATTN T. N. DAVIS (UNCL ONLY)
    01CY  ATTN NEAL BROWN (UNCL ONLY)
    01CY  ATTN TECHNICAL LIBRARY

GTE SYLVANIA, INC.
ELECTRONICS SYSTEMS GRP-EASTERN DIV
77 A STREET
NEEDHAM, MA 02194
    01CY  ATTN MARSHAL CROSS

ILLINOIS, UNIVERSITY OF
DEPARTMENT OF ELECTRICAL ENGINEERING
URBANA, IL 61803
    01CY  ATTN K. YEH

ILLINOIS, UNIVERSITY OF
107 COBLE HALL
801 S. WRIGHT STREET
URBANA, IL 60680
    (ALL CORRES ATTN SECURITY SUPERVISOR FOR)
    01CY  ATTN K. YEH

22

INSTITUTE FOR DEFENSE ANALYSES
400 ARMY-NAVY DRIVE
ARLINGTON, VA 22202
    01CY ATTN J. M. AEIN
    01CY ATTN ERNEST BAUER
    01CY ATTN HANS WOLFHARD
    01CY ATTN JOEL BENGSTON

HSS, INC.
2 ALFRED CIRCLE
BEDFORD, MA 01730
    01CY ATTN DONALD HANSEN


INTL TEL & TELEGRAPH CORPORATION
500 WASHINGTON AVENUE
NUTLEY, NJ 07110
    01CY ATTN TECHNICAL LIBRARY


JAYCOR
1401 CAMINO DEL MAR
DEL MAR, CA 92014
    01CY ATTN S. R. GOLDMAN


JOHNS HOPKINS UNIVERSITY
APPLIED PHYSICS LABORATORY
JOHNS HOPKINS ROAD
LAUREL, MD 20810
    01CY ATTN DOCUMENT LIBRARIAN
    01CY ATTN THOMAS POTEMRA
    01CY ATTN JOHN DASSOULAS

LOCKHEED MISSILES & SPACE CO INC
P. O. BOX 504
SUNNYVALE, CA 94088
    01CY ATTN DEPT 60-12
    01CY ATTN D. R. CHURCHILL

LOCKHEED MISSILES AND SPACE CO INC
3251 HANOVER STREET
PALO ALTO, CA 94304
    01CY ATTN MARTIN WALT DEPT 52-10
    01CY ATTN RICHARD G. JOHNSON DEPT 52-12
    01CY ATTN W. L. IMHOF DEPT 52-12

KAMAN SCIENCES CORP
P. O. BOX 7463
COLORADO SPRINGS, CO 80933
    01CY ATTN T. MEAGHER

LINKABIT CORP
10453 ROSELLE
SAN DIEGO, CA 92121
    01CY ATTN IRWIN JACOBS

M.I.T. LINCOLN LABORATORY
P. O. BOX 73
LEXINGTON, MA 02173
    01CY ATTN DAVID M. TOWLE
    01CY ATTN P. WALDRON
    01CY ATTN L. LOUGHLIN
    01CY ATTN D. CLARK

MARTIN MARIETTA CORP
ORLANDO DIVISION
P. O. BOX 5837
ORLANDO, FL 32805
    01CY ATTN R. HEFFNER

MCDONNELL DOUGLAS CORPORATION
5301 BOLSA AVENUE
HUNTINGTON BEACH, CA 92647
    01CY ATTN N. HARRIS
    01CY ATTN J. MOULE
    01CY ATTN GEORGE MROZ
    01CY ATTN W. OLSON
    01CY ATTN R. W. HALPRIN
    01CY ATTN TECHNICAL LIBRARY SERVICES

MISSION RESEARCH CORPORATION
735 STATE STREET
SANTA BARBARA, CA 93101
    01CY ATTN P. FISCHER
    01CY ATTN W. F. CREVIER
    01CY ATTN STEVEN L. GUTSCHE
    01CY ATTN D. SAPPENFIELD
    01CY ATTN R. BOGUSCH
    01CY ATTN R. HENDRICK
    01CY ATTN RALPH KILB
    01CY ATTN DAVE SOWLE
    01CY ATTN F. FAJEN
    01CY ATTN M. SCHEIBE
    01CY ATTN CONRAD L. LONGMIRE
    01CY ATTN WARREN A. SCHLUETER

MITRE CORPORATION, THE
P. O. BOX 208
BEDFORD, MA 01730
    01CY ATTN JOHN MORGANSTERN
    01CY ATTN G. HARDING
    01CY ATTN C. E. CALLAHAN

MITRE CORP
WESTGATE RESEARCH PARK
1820 DOLLY MADISON BLVD
MCLEAN, VA 22101
    01CY ATTN W. HALL
    01CY ATTN W. FOSTER

PACIFIC-SIERRA RESEARCH CORP
1456 CLOVERFIELD BLVD.
SANTA MONICA, CA 90404
    01CY ATTN E. C. FIELD JR

PENNSYLVANIA STATE UNIVERSITY
IONOSPHERE RESEARCH LAB
318 ELECTRICAL ENGINEERING EAST
UNIVERSITY PARK, PA 16802
    (NO CLASSIFIED TO THIS ADDRESS)
    01CY ATTN IONOSPHERIC RESEARCH LAB

PHOTOMETRICS, INC.
442 MARRETT ROAD
LEXINGTON, MA 02173
    01CY ATTN IRVING L. KOFSKY

PHYSICAL DYNAMICS INC.
P. O. BOX 3027
BELLEVUE, WA 98009
    01CY ATTN E. J. FREMOUW

PHYSICAL DYNAMICS INC.
P. O. BOX 10367
OAKLAND, CA. 94610
    ATTN: A. THOMSON

R & D ASSOCIATES
P. O. BOX 9695
MARINA DEL REY, CA 90291
    01CY ATTN FORREST GILMORE
    01CY ATTN BRYAN GABBARD
    01CY ATTN WILLIAM B. WRIGHT JR
    01CY ATTN ROBERT F. LELEVIER
    01CY ATTN WILLIAM J. KARZAS
    01CY ATTN H. ORY
    01CY ATTN C. MACDONALD
    01CY ATTN R. TURCO

RAND CORPORATION, THE
1700 MAIN STREET
SANTA MONICA, CA 90406
    01CY ATTN CULLEN CRAIN
    01CY ATTN ED BEDROZIAN

RIVERSIDE RESEARCH INSTITUTE
80 WEST END AVENUE
NEW YORK, NY 10023
    01CY ATTN VINCE TRAPANI

24

PLEASE DISTRIBUTE ONE COPY TO EACH OF THE FOLLOWING PEOPLE:

ADVANCED RESEARCH PROJECTS AGENCY (ARPA)
STRATEGIC TECHNOLOGY OFFICE
ARLINGTON, VIRGINIA

    CAPT. DONALD M. LEVINE

NAVAL RESEARCH LABORATORY
WASHINGTON, D.C.  20375

    DR. P. MANGE
    DR. R. MEIER
    DR. E. SZUSZCZEWICZ - CODE 4127

    DR. J. GOODMAN - CODE 7560

SCIENCE APPLICATIONS, INC.
1250 PROSPECT PLAZA
LA JOLLA, CALIFORNIA  92037

    DR. D. A. HAMLIN
    DR. L. LINSON
    DR. D. SACHS

DIRECTOR OF SPACE AND ENVIRONMENTAL LABORATORY
NOAA
BOULDER, COLORADO  80302

    DR. A. GLENN JEAN
    DR. G. W. ADAMS
    DR. D. N. ANDERSON
    DR. K. DAVIES
    DR. R. F. DONNELLY

A. F. GEOPHYSICS LABORATORY
L. G. HANSOM FIELD
BEDFORD, MASS.  01730

    DR. T. ELKINS
    DR. W. SWIDER
    MRS. R. SAGALYN
    DR. J. M. FORBES
    DR. T. J. KENESHEA
    DR. J. AARONS

OFFICE OF NAVAL RESEARCH
800 NORTH QUINCY STREET
ARLINGTON, VIRGINIA  22217

    DR. H. MULLANEY

COMMANDER
NAVAL ELECTRONICS LABORATORY CENTER
SAN DIEGO, CALIFORNIA  92152

    DR. M. BLEIWEISS
    DR. I. ROTHMULLER
    DR. V. HILDEBRAND
    MR. R. ROSE

U. S. ARMY ABERDEEN RESEARCH AND DEVELOPMENT CENTER
BALLISTIC RESEARCH LABORATORY
ABERDEEN, MARYLAND

    DR. J. HEIMERL

COMMANDER
NAVAL AIR SYSTEMS COMMAND
DEPARTMENT OF THE NAVY
WASHINGTON, D.C.  20360

    DR. T. CZUBA

HARVARD UNIVERSITY
HARVARD SQUARE
CAMBRIDGE, MASS.  02138

    DR. M. B. MCELROY
    DR. R. LINDZEN

PENNSYLVANIA STATE UNIVERSITY
UNIVERSITY PARK, PENNSYLVANIA  16802

    DR. J. S. NISBET
    DR. P. R. ROHRBAUGH
    DR. D. E. BARAN
    DR. L. A. CARPENTER
    DR. M. LEE
    DR. R. DIVANY
    DR. P. BENNETT
    DR. E. KLEVANS

UNIVERSITY OF CALIFORNIA, LOS ANGELES
405 HILLGARD AVENUE
LOS ANGELES, CALIFORNIA  90024

    DR. F. V. CORONITI
    DR. C. KENNEL

UNIVERSITY OF CALIFORNIA, BERKELEY
BERKELEY, CALIFORNIA  94720

    DR. M. HUDSON

UTAH STATE UNIVERSITY
4TH N. AND 8TH STREETS
LOGAN, UTAH  84322

    DR. P. M. BANKS
    DR. R. HARRIS
    DR. V. PETERSON
    DR. R. MEGILL
    DR. K. BAKER

CORNELL UNIVERSITY
ITHACA, NEW YORK  14850

    DR. W. E. SWARTZ
    DR. R. SUDAN
    DR. D. FARLEY
    DR. M. KELLEY

NASA
GODDARD SPACE FLIGHT CENTER
GREENBELT, MARYLAND  20771

    DR. S. CHANDRA
    DR. K. MAEDO

# END

## DATE
## FILME

# I-8

## DTIC